https://doi.org/10.5194/essd-2020-324
Preprint. Discussion started: 22 January 2021

Open Access Earth System Science Data Discussions

Slope deformation, reservoir variation and meteorological data at the Khoko landslide, Enguri hydroelectric basin (Georgia), during 2016-2019

Alessandro Tibaldi[1*], Federico Pasquaré Mariotto[2], Paolo Oppizzi[3], Fabio Luca Bonali[1], Nino Tsereteli[4], Levan Mebonia[5], Johni Chania[5]

[1] Department of Earth and Environmental Sciences, University of Milan Bicocca, 20129 Milan, Italy
[2] Department of Human and Innovation Sciences, Insubria University, Como, Italy
[3] Geolog.ch, Mendrisio, Switzerland
[4] Institute of Geophysics, University of Tbilisi, Tbilisi, Georgia
[5] Enguresi LtD Society, Georgia

***Corresponding Author**: alessandro.tibaldi@unimib.it

Abstract

The Greater Caucasus mountain belt is characterized by deep valleys, steep slopes and frequent seismic activity, the combination of which results in major landslide hazard. Along the eastern side of the Enguri water reservoir lies the active Khoko landslide, whose head scarp zone affects the important Jvari-Khaishi-Mestia road, one of the few connections with the interior of the Greater Caucasus. Here, we present a database of measurement time series taken over a period of 4 years (2016-2019) that enable to compare slope deformation with meteorological factors and man-induced perturbations owing to variations in the water level of the reservoir. The monitoring system we used is composed of two digital extensometers, placed within two artificial trenches excavated across the landslide head scarp. The stations are equipped also with internal and near ground surface thermometers. The data set is integrated by daily measurements of rainfall and lake level. The monitoring system was set up in the framework of a NATO-funded project, aimed at assessing different types of geohazards affecting the Enguri artificial reservoir and the related hydroelectrical plant. Our results indicate that the Khoko landslide displacements appear to be controlled by variations in hydraulic load, in turn induced by lake level oscillations, with a delay of months between lake infilling and extension rate increase. Rainfall and temperature variations do not seem to affect slope deformations. The full databases are freely available online at DOI: 10.20366/unimib/unidata/SI384-1.1 (Tibaldi et al., 2020).

1 Introduction

Landslides are widespread natural hazard sources, affecting most of the world's countries and capable of causing serious economic losses. In fact, they can damage buildings, communication systems and the overall environment. Moreover, such natural events are major sources of loss of life (Froude and

https://doi.org/10.5194/essd-2020-324
Preprint. Discussion started: 22 January 2021

Petley, 2018). The monitoring of landslides is a necessary step to implement protective measures, as it allows to recognize possible acceleration in slope deformation rate, to alert residents or close road communication systems, where needed. This type of monitoring is also of paramount importance for assessing possible triggering factors (Casagli et al., 2009), determining the level of risk (Spiker and Gori, 2003), and planning land use and risk management (Fell et al., 2005; Bertolini et al., 2005). This activity can be of special relevance in case of complex situations, such those affecting an artificial water reservoir, where water variations can destabilize (or stabilize) the slopes overlooking the basin. In such a case, multiparameter data can be crosscut in order to look for possible correlations between lake level variations, meteorological conditions, and slope deformations, which in turn are key to effectively managing the filling and emptying of the reservoir.

The database of slope deformation can be derived from a variety of possible monitoring tools, which range from on-site instruments to remotely controlled ones. The former include continuous or intermittent data collection, such as settlement gauges, inclinometers and piezometric groundwater measurements (Liu and Wang, 2008). Surveys can be carried out by means of detection of the surface movements of unstable area by means of levels, theodolites, Electronic Distance Measurement, and total station GPS measurements (Liu Shao-tang, 2006). Remote control systems include aerial or terrestrial photogrammetry in the visible or radar ranges (Bitelli et al., 2004). Monitoring the distance between two points across the main landslide head scarp is the most suitable way to describe the displacements within the landslide, at a site far away from its toe. This is particularly helpful in assessing the susceptibility of the whole landslide body to variations in toe conditions: In fact, a feedback at the head scarp helps decipher the long range of these effects.

In November 2016, an international team of scientists, under the aegis of NATO, set about working in the area of the Enguri artificial water reservoir, on the southwestern foothills of the Greater Caucasus, Georgia (Fig. 1). During the first of several research missions, the team installed two digital extensometers across the head scarp of the major, active Khoko landslide, located along the eastern mountain slope overlooking the reservoir. The associated hydroelectrical plant, built during the Soviet era (Fig. 1c), is responsible for about half of the energy supply to the country (Tibaldi et al. 2018). This monitoring activity is particularly relevant because the study area is located in a region affected by widespread seismicity (Fig. 1a), owing to still active mountain building processes, which have led to the formation of the Greater and Lesser Caucasus, resulting from the continent–continent collision between the African–Arabian and Eurasian plates (Reilinger 1997; 2006; Koçyigit et al. 2001; Pasquaré et al. 2011). Seismicity can produce earthquake with Ms of 6-7 (Tsereteli et al., 2016) and macroseismic intensities up to 10 (Varazanashvili et al., 2018), as a consequence of active compressional tectonics (Tsereteli et al., 2016; Tibaldi et al., 2017a, b, 2019). As broadly agreed upon

https://doi.org/10.5194/essd-2020-324
Preprint. Discussion started: 22 January 2021


Open Access Earth System Science Data Discussions

in the scientific literature, there exists a tight connection between active tectonic processes and the occurrence of landslides (e.g. Tibaldi et al. 2004, 2015; Tibaldi and Pasquaré, 2008; Pasquaré Mariotto and Tibaldi, 2016). As it is beyond doubt that, in the future, a seismic event will happen again in the area, the installed monitoring landslide system will be instrumental in quantitatively assessing the effects of ground shaking on slope deformation rate.

Last but not least, the Jvari-Khaishi-Mestia road cuts across the uppermost portion of the Khoko landslide, along a 2-km-long stretch, at an elevation of 700 m a.s.l. Several field surveys in the area enabled the team to report the presence of developing cracks, shear planes, opening of holes, and an overall active deformation concentrated on 150-200-m-long road segments, which could pose serious threats to road traffic safety. Such fracture zones are being continuously repaired by way of asphalt refilling, with the purpose of preventing serious damage and incidents.

We hereby provide and illustrate the database of measurements gathered by means of the integrated monitoring system installed at the Khoko landslide. The main goals of our research are to identify range and patterns of deformation, and to assess possible relations between changes in water level at the artificial Enguri reservoir, meteorological factors (temperature and rain) and slope deformations. Analysis of these multi-temporal datasets is of broader interest as it can provide a detailed framework for planning the most appropriate actions in the management of major water reservoirs aimed at energy production.

https://doi.org/10.5194/essd-2020-324
Preprint. Discussion started: 22 January 2021

Open Access Earth System Science Data Discussions

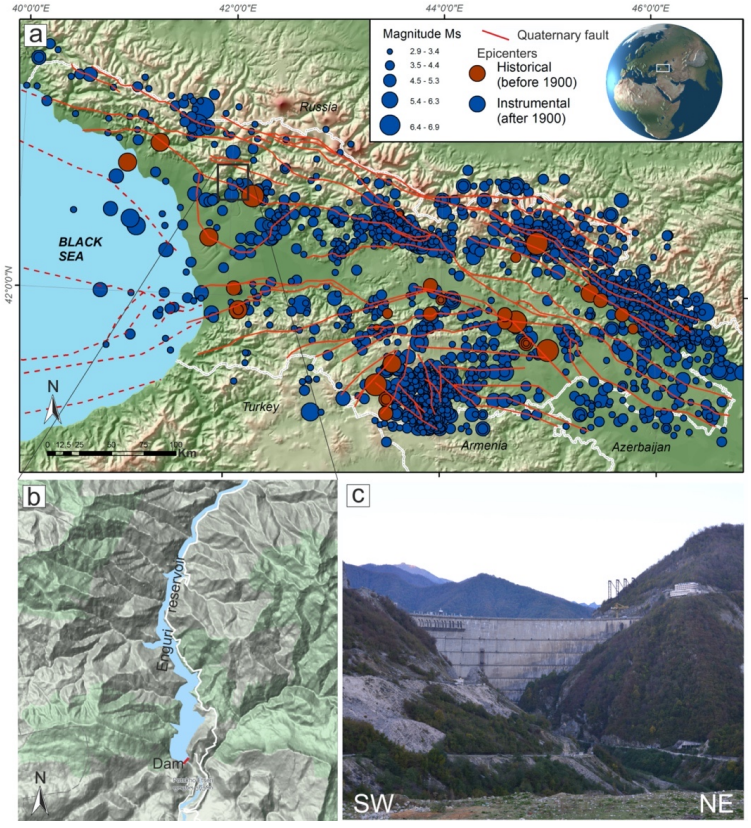

Figure 1. *(a) Main historic and instrumental earthquake epicenters in the western Greater Caucasus; the black rectangle shows the area of Figure (b), white lines are country borders, the main Quaternary faults (red lines) are from Gulen et al. (2011) and Tsereteli et al. (2016). Reference system: WGS84 / geographic coordinates. (b) DEM of the Enguri reservoir area, with dam location, © Google Maps. (c) Photo of the Enguri dam.*

2 Site description

The study area is characterized by substrate rocks and widespread Quaternary deposits. Around the landslide area, there is the presence of Jurassic volcanic and terrigenous rocks and Cretaceous carbonate deposits (Fig. 2), generally dipping to the south. The dip of the Cretaceous strata cropping out around the Enguri dam is in the order of 60-70°, whereas the bedding attains a shallower dip northward, becoming sub-horizontal toward the northern part of the Enguri reservoir. Below the carbonate layers, Jurassic deposits can be observed, made of sandstones, tuffs, tuff-breccia and gypsum layers that locally crop out along the southeastern slopes of the reservoir.

The studied slope is marked by landforms that are typical of recent/active gravitational deformation; the total surface area affected by slope instability, which is about 1.2 km^2, is characterized by widespread debris deposits, ancient landslide deposits (Fig. 2), and fractured rocks. At an altitude of

https://doi.org/10.5194/essd-2020-324
Preprint. Discussion started: 22 January 2021


Open Access Earth System Science Data Discussions

720-740 m, a number of scarps can be noticed, facing westward and located along the Jvari-Khaishi-Mestia road (Figs. 2 and 3). The height of such scarps ranges from 20 m to 70 m. At the foot of the scarps, the topography is either horizontal or gently dipping westward, suggesting a possible area of uphill tilting of the slope (Fig. 3a). The asphalted surface of the road here is affected by fissures, as wide as a few centimeters, and by westward-facing, 20-cm-high (in 2016) scarps (Fig. 3d). These structures are parallel to sub-parallel to the morphological high head scarps. As documented by Tibaldi et al. (2019), in the forest across the southern segment of the head scarps, tens of meters long, and up to 3.8 m wide fissures were found. Some of the trees, with trunks of about 20 cm in diameter, grew inside the fissures, suggesting that the fissures have a long history, at least dating back to several tens of years (Tibaldi et al., 2019).

Downhill from the head scarp zone, several changes of inclination affect the slope, resulting in a series of downhill-facing scarps. Most are oriented perpendicularly to the local slope dip and are located in the upper part of the slope. This suggests the possible presence of secondary landslide slip planes (Tibaldi et al., 2019). Besides, most of the studied slope is characterized by the presence of several tilted trees; moreover, locally 100% of trunks are tilted, and this is another indicator of active slope deformation (Fig. 3c).

The arrangement of river streams, as shown Figure 2, is based on the present-day river network and Soviet topographic maps compiled before the build-up of the water reservoir. In the slope section above the present-day lake, the rivers mostly follow the average slope dip, according to a dendritic pattern. Below the present-day lake level, one single river was draining the landslide area. Here, at the toe of the slope, this single river was running parallel to the main Enguri river but with a northward, opposite flow (Tibaldi et al., 2019). This is an anomaly in the river pattern that can be linked to a disturbance in the average slope topography, suggesting a possible early bulging of the landslide toe.

https://doi.org/10.5194/essd-2020-324
Preprint. Discussion started: 22 January 2021

Open Access Earth System Science Data Discussions

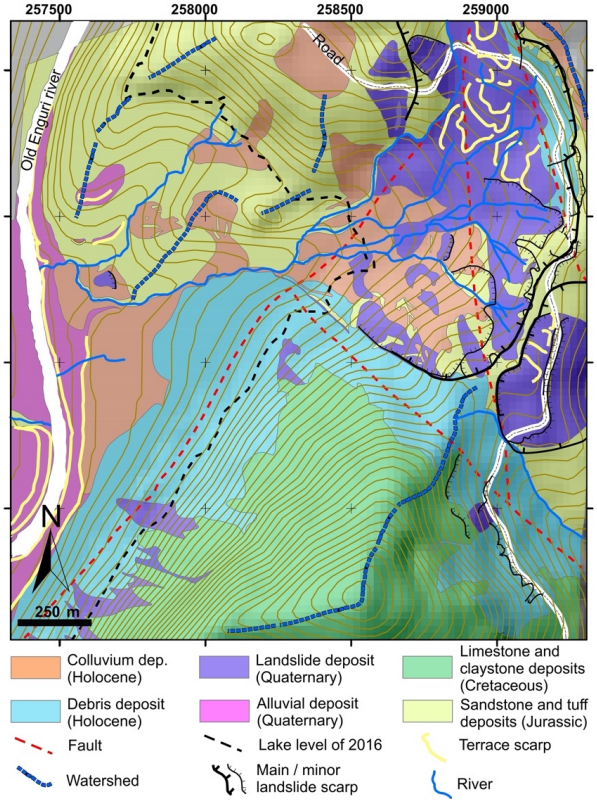

134

135 ***Figure 2.*** *Geological and geomorphological map of the study area, redrawn after* Tibaldi et al. (2019).

136

https://doi.org/10.5194/essd-2020-324
Preprint. Discussion started: 22 January 2021

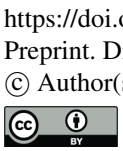

Open Access Earth System Science Data Discussions

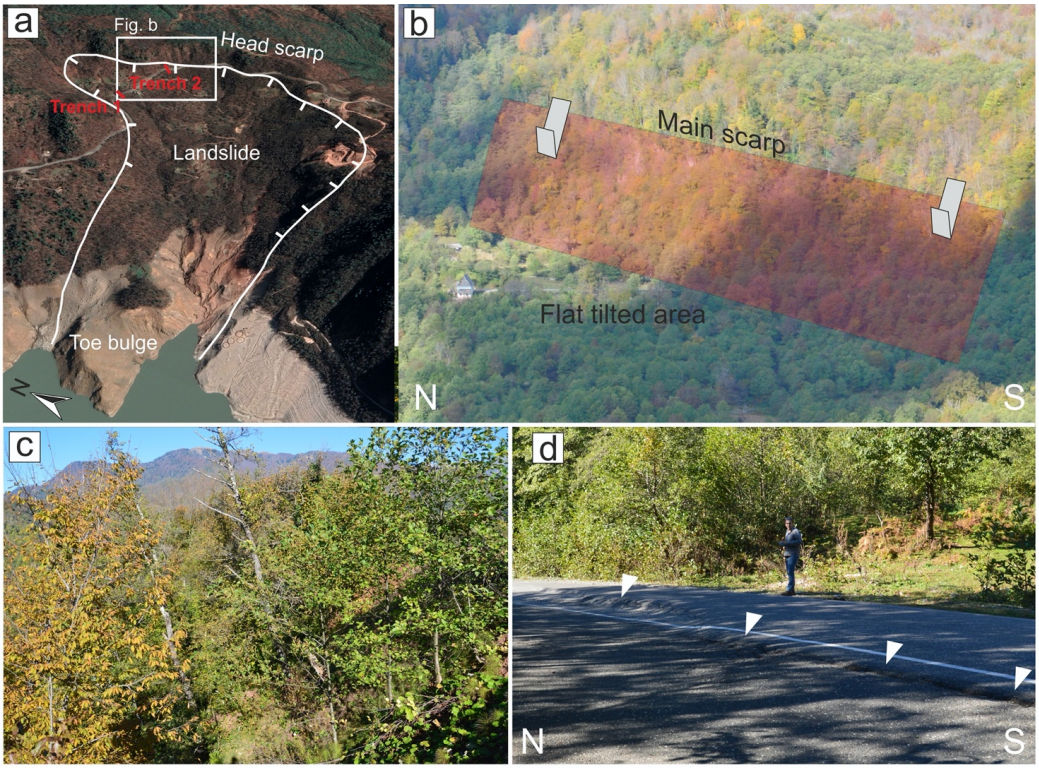

137

138 ***Figure 3.*** *(a) Oblique view of the studied landslide (© Google Earth); trench locations are shown.*
139 *(b) Photo of a segment of the landslide head scarp; it is worth noting the flat-lying area at the foot of*
140 *the scarp, created by uphill tilting of the slope during rotational movements of the landslide block.*
141 *House for scale (to the left side of the flat area). (c) Example of tilted trees along the landslide slope.*
142 *(d) Photo of the escarpments cutting the Jvari-Khaishi-Mestia road (white triangles), representing*
143 *the surface expression of active landslide slip planes.*

144

145 **3 Methodology and instrumentation**

146 In 2016, two trenches were excavated across the main head scarps of the Khoko landslide. The
147 location of the sites selected for trenching is indicated in Figure 3a, and these locations were based
148 upon the presence of clear indicators of active deformation on the road, at the foot of the main
149 landslide scarps. Each of the two trenches was suitable for hosting a horizontal, digital extensometer
150 (Wire Linear Potentiometric Transducer, SF500). The two trenches were opened perpendicularly to
151 the scarp strike, crossing the road at a high angle (Fig. 4a). The instrumentation was placed within a
152 protection system aimed at avoiding disturbance or damage from heavy load traffic (Figs. 4b-d). The
153 opening of the trenches was performed in two stages, so as to enable vehicles to drive through the

https://doi.org/10.5194/essd-2020-324
Preprint. Discussion started: 22 January 2021

area along alternating lanes. The protection of the measurement stations consists of a channel in reinforced concrete, buried down to a depth of at least 50 cm.

The instrument is composed of a wire, a digital meter, and a recorder system. The stainless steel wire changes its length based on the relative movements of the piercing points to which it is connected. The wire was inserted into a pipe, laid down horizontally and protected with sand (Fig. 4c-d). At both ends, steel pipes were positioned, aimed at securing the measurement wire and the electronic instrumentation. Each vertical tube was equipped with a steel cover and gasket. The two covers were buried underneath a 15 cm-thick soil layer. These operations were made more difficult by the presence of a pavement in concrete beneath the present-day asphalt layer. The meter is a wire potentiometric position transducer that turns a linear motion into a resistance variation. It is made of a precision rotating potentiometer operated by the winding or unwinding stainless steel wire.

Due to the impossibility of transmitting the data directly to a computer at the Enguri dam premises or via internet (due to the remoteness of the site), the measurements have been stored in a digital recorder (data logger THEMIS-USB-GPRS) and downloaded on a 30-day basis. The system is connected to a set of insulated batteries with an autonomy of 6 months.

Extensometer n. 1 was put in operation in November 2016, whereas the second extensometer began recording data in May 2017. The instruments include also an internal and external sensor of temperature - PT100.

The station for measuring the Enguri lake level is installed at an altitude of 360 m in the dam. It is made of a Multi-Channel Recorder RSG30 Ecograph T, by Endress+Hauser, using the Software ETU00xA, V2.02.xx. The data are transmitted in real-time to the dam administration and stored in local computers.

Rainfall amounts are recorded by a station, situated at an altitude of 540 m near the dam's administrative building. The station features the Davis Vantage Pro2 instrument, suitable for measuring rainfall, wind speed, temperature and humidity, with data updated every 2.5 seconds. It comes with a self-emptying tipping spoon determining rainfall amounts in 0.2 mm increments, and is laser-calibrated for increasing accuracy. The data are transmitted in real-time to the dam administration and stored in local computers.

https://doi.org/10.5194/essd-2020-324
Preprint. Discussion started: 22 January 2021

Figure 4*. (a) Opening of trench n. 1. (b) Installation of the concrete protection for the extensometer. (c) Section transversal to the extensometer system. (d) Longitudinal section of the extensometer system. Location of the two measurement stations provided in Figure 3a.*

4 Results

4.1 Extensometer data

In Figure 5 are shown the readings collected over a 35-month interval, between the 4th November 2016 and 9 October 2019, by the extensometer at station n. 1. The overall extension recorded during the 35-month period, 88.7 mm, gives an average extension rate of 0.08 mm/day or 30.8 mm/y. Deformation peaked from 16 May 2017 to 8 August 2017, with a total extension of 52 mm, corresponding to an average rate of 0.61 mm/day. This documented acceleration in the movement coincided with the opening of new fractures on the road surface at about 700 m of altitude, i.e. 230 m above the average lake level of 470 m a.s.l. For comparison,

https://doi.org/10.5194/essd-2020-324
Preprint. Discussion started: 22 January 2021

From 3 October 2017, deformation ceased until 16 January 2018. This date marks the beginning of another period of slight deformation, lasting until 6 March 2018. From this date on, another interval of deformation rate increase was recorded, although much less pronounced than the previous one. This increase lasted until 22 May 2018, marked by a rate of 0.12 mm/day. From the end of May 2018 to October 2019, deformation was linear, with a data gap between 30/12/2018 and 13/8/2019 due to a technical problem. This slower, creep-like movement was accompanied by the development of small sinkholes and fractures within the landslide body.

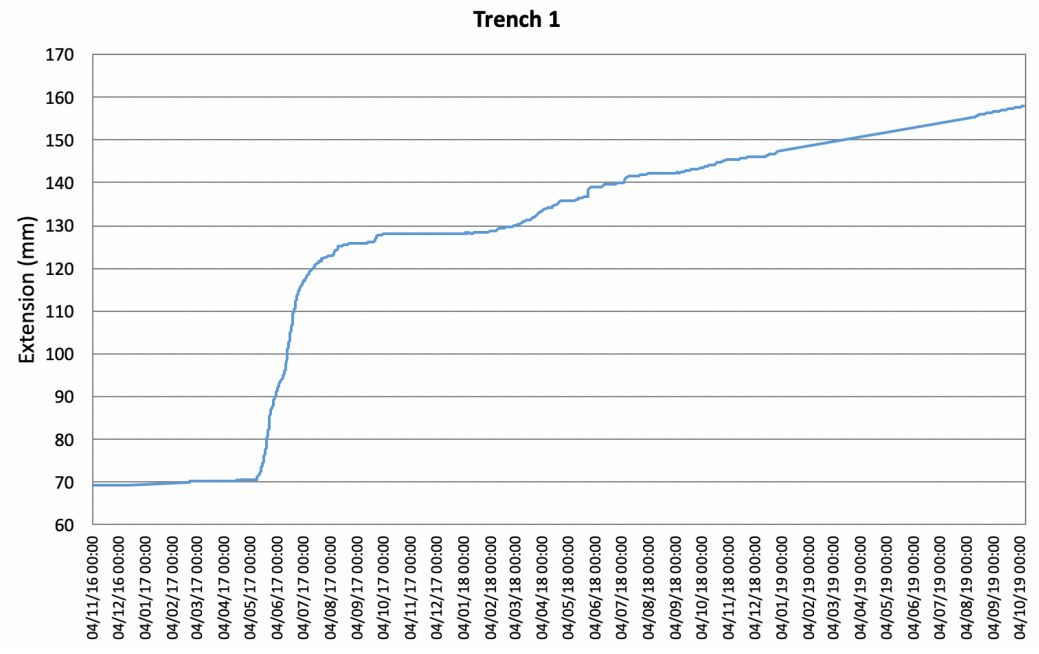

Figure 5. *Graph showing the readings of the incremental extension (in mm), associated with landslide surface displacement, and recorded at station n.1 from November 2016 to October 2019 .*

At extensometer n. 2, data are shown over a 28.5-month interval (from 18 May 2017 to 30 September 2019) (Fig. 6). Here, the total amount of deformation was 19.14 mm, with an average extension rate of 0.02 mm/day or 8.17 mm/y. From the beginning until 24 October 2017, there was a steady slight deformation, followed by a period of high deformation expressed, in the graph, by a line with an upward convexity, indicating firstly a strong increase and later on a gradual decrease in the extension rate. This period lasted until 27 February 2018 and was characterized by an average rate of 0.16 mm/day, followed by another increase for one month, and then by a steady deformation until 15

https://doi.org/10.5194/essd-2020-324
Preprint. Discussion started: 22 January 2021

November 2018. Thereafter, until 29 January 2019, a new increase in the extension rate was observed, after which deformation ceased.

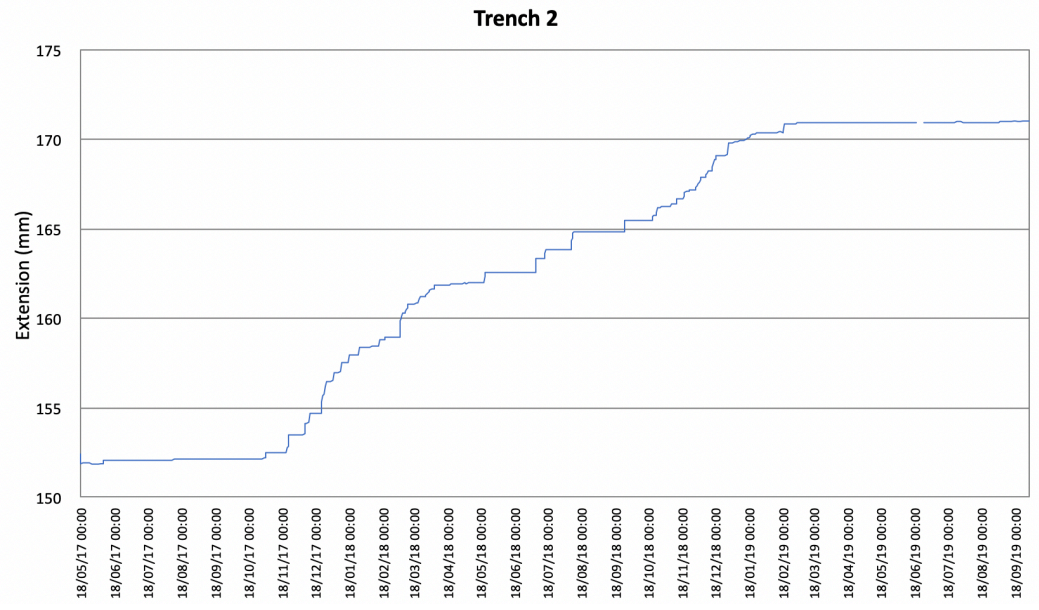

Figure 6. *Graph showing the readings of the incremental extension (in mm), associated with landslide surface displacement, and recorded from May 2017 to September 2019 at station n.2.*

4.2 Meteorological data

The amount of rainfall shows important variations (Fig. 7). Rainy days are mostly characterized by amounts within 10-20 mm/day. Peaks of 40-50 mm/day appear on 7/9/17, 5/2/18, 12/2/18, 26/9/18, 23/5/20 and 18/6/20. Peaks between 51-60 mm/day occurred on 6/12/17, 5/3/18 and 1/12/19. The highest peaks, above 70 mm/day occurred on 22/10/18 and 25/7/19. Periods of particularly heavy rains took place from 19/1/18 to 12/5/18 and from 22/9/18 to 16/1/19. From middle April 2018 to 25 September 2018 there has been a gap in data due to technical problems.

In regard to temperatures (T), these show a double fluctuation (Fig. 8); the short-term fluctuation took place within a frequency of 5-20 days, whereas the long term fluctuation developed each 12 months. At Trench 1, in the first period of observations, the T at the data logger, near the ground surface, gradually decreased to 3° on 22/2/17, although there has been a gap in data, due to a technical problem, from half of December 2017 to half of February 2017. Then T increased until it peaked to 22,9° on 15/8/17. From this date until 2/2/18, there was a gradual decrease, reaching a minimum of 5.5°. Then T increased again, when it reached a maximum value of 22.4° on 10/8/18. The T then

https://doi.org/10.5194/essd-2020-324
Preprint. Discussion started: 22 January 2021

237 decreased down to 0.9° on 27/12/18. At Trench 2 the variation of T was similar to Trench 1, although
238 the absolute values were sometime higher of 1-2°.
239 The T of the wire inside the instrument recorded the same pattern of variations, although smoothed,
240 with T systematically higher in the order of 3-4° at Trench 1, and with a much smaller difference at
241 Trench 2 (Fig. 8).
242

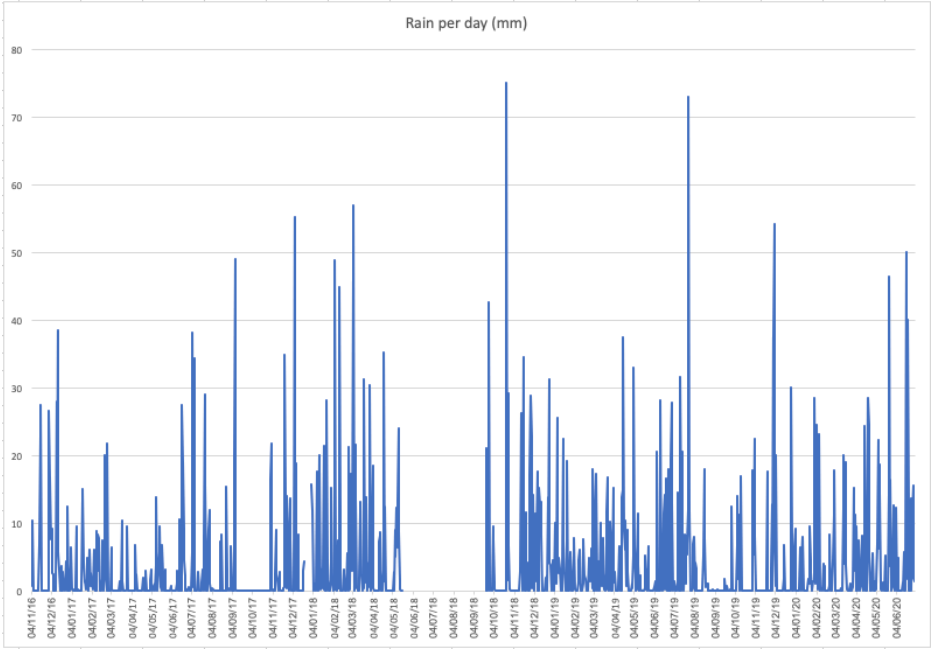

243
244 ***Figure 7.*** *Amount of rainfall recorded near the landslide, from 4 November 2016 to 30 June 2020.*
245

https://doi.org/10.5194/essd-2020-324
Preprint. Discussion started: 22 January 2021

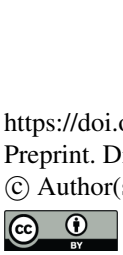

Open Access Earth System Science Data Discussions

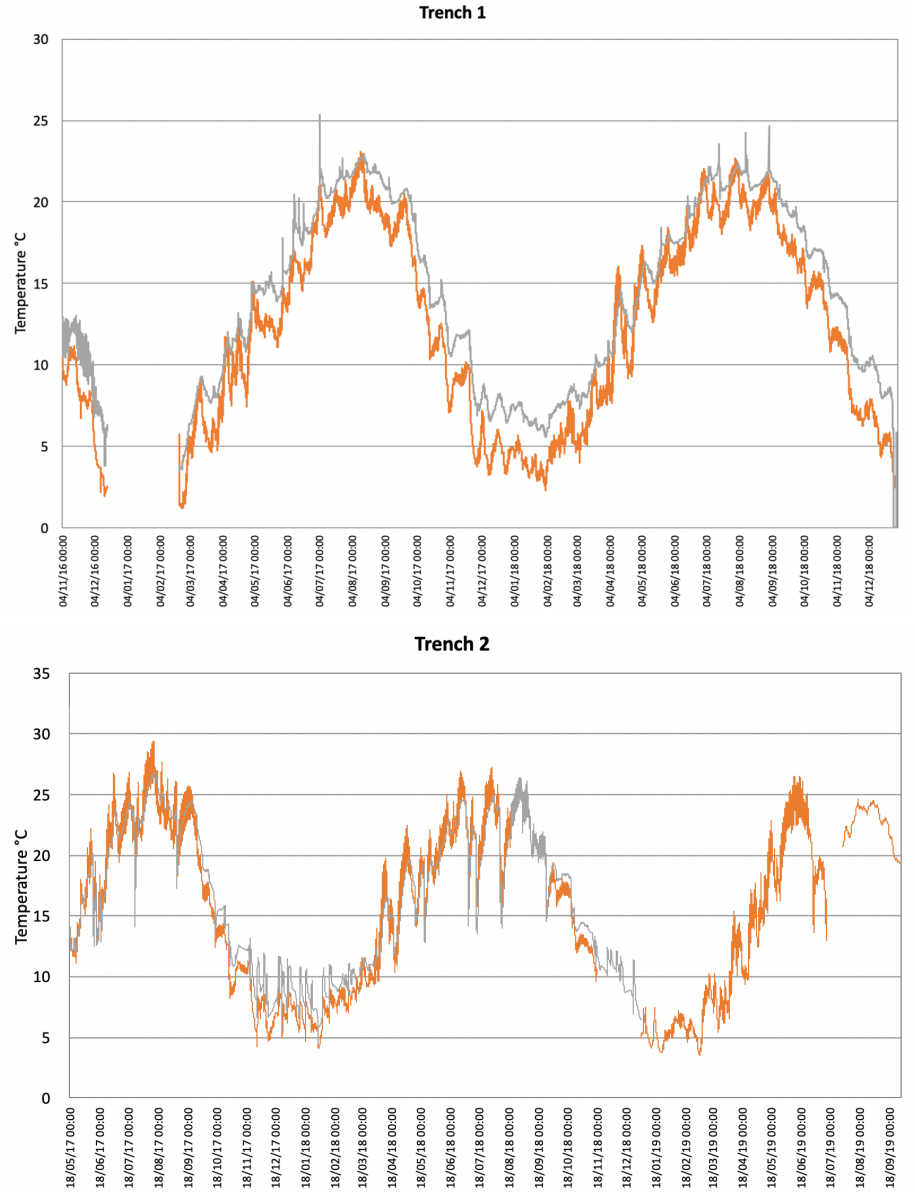

Figure 8. *Temperatures recorded at Trench 1 from November 2016 to December 2018, and at Trench 2 from May 2017 to September 2019. The grey line represents the variations in temperature of the extensometer wire, inside the instrument, whereas the orange line shows temperature variations at the data logger that is near the ground surface.*

https://doi.org/10.5194/essd-2020-324
Preprint. Discussion started: 22 January 2021

4.3 Lake level data

Since the beginning of our measurements (1 January 2017) until 20 February 2017, there was a continuous emptying of the reservoir, the level of which dropped down to a minimum of 410 m a.s.l. (Fig. 9). Thereafter, the reservoir was filled again, to a maximum of 510 m on 5 August 2017, followed by a further increase on 12 September 2017, up to 511 m. Since this date on there was a decrease of the lake level until 29 February 2018, when the lake's level reached an altitude of 443 m. Then, it increased again reaching the altitude of 510 m on 30 June 2018. Later on, a new period of level decrease lasted until 31 March 2019, when it reached 414 m. Over the next month there was an oscillation with an increase of 35 m followed by a decrease. From 23 April 2019, a lake level increase was recorded, which ended on 26 July 2019, reaching an altitude of 507 m. Thereafter, a new period of lake level decrease took place, until 29 April 2020 when it reached 419 m.

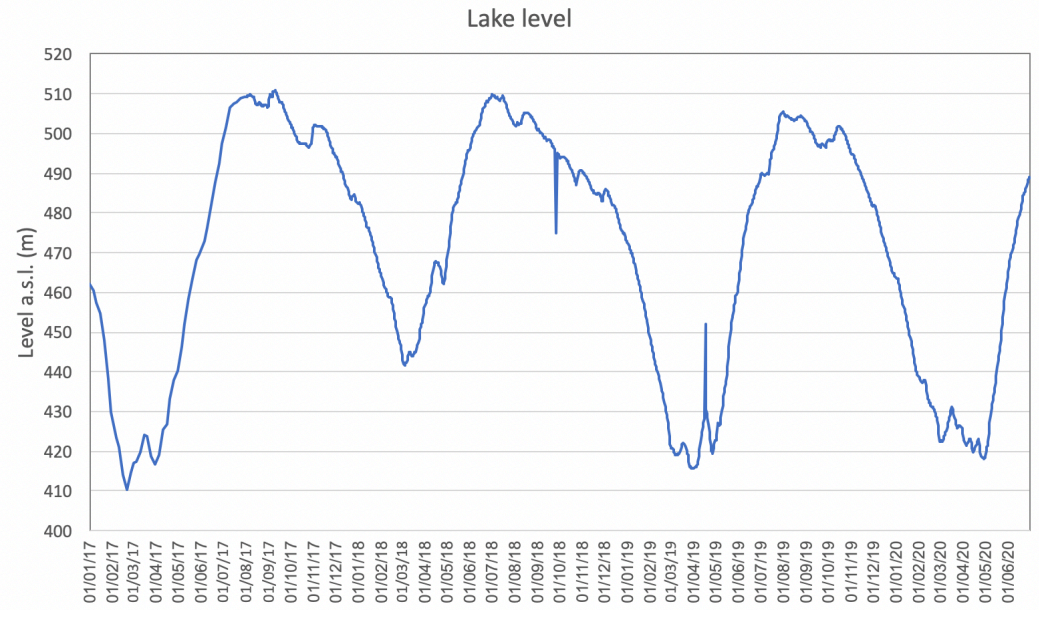

Figure 9. *Variations of the level of the Enguri artificial water reservoir from 1 January 2017 to 30 June 2020.*

5 Discussion

Here, we briefly discuss all the data, which we have combined in the graphs of Figure 10, so as to provide a more immediate interpretation. At extensometer n. 1, the total amount of deformation has been 88.7 mm in 35 months, yielding an average extension rate of 0.08 mm/day or 30.8 mm/y. Deformation peaked from 16 May 2017 to 8 August 2017, with a total extension of 52 mm that

https://doi.org/10.5194/essd-2020-324
Preprint. Discussion started: 22 January 2021

corresponds to a rate of 0.61 mm/day, about eight times the average extension rate during the whole measurement period. This extension rate increase follows the almost complete drawdown of the lake (which went down to the lowest level on 21 February 2017) and the ensuing period of lake level infilling, with a 100-m water level increase. A delay of about one month can be recognized between the lake level increase and the deformation rate increase. Another interval of extensional rate increase, although much smoother than the previous one, is recognizable for a period after 6 March 2018, at the same time as a 67-m increase of the water level. During the third period of lake filling and refilling, due to technical problems at the extensometer, possible further rate variations were not recorded. During periods of water level lowering, instead, the extension rate tends to decrease to the lowest values. The amount of rainfall and temperature variations do not correlate with the extension rate values.

At extensometer n. 2, the total amount of deformation was 19.14 mm in 28.5 months, with an average extension rate of 0.02 mm/day or 8.17 mm/y. Deformation increased, from 31 October 2017 to 1 April 2018, to 0.13 mm/day, corresponding to a 5-month interval of increased deformation, in a much similar way as what was recorded at extensometer n. 1, over a three-month period. Another period of sustained deformation took place from 25 September 2018 to 28 December 2018. It is worth noting that the deformation curves derived from the two extensometers have a similar shape, but at extensometer n. 2 the curve is shifted onward by four to six months. This means that, at extensometer n. 2, the delay between lake filling and slope reaction is longer than at the other extensometer.

As documented by Tibaldi et al. (2019), based on the analysis of the Quaternary geological deposits of the area, and by the presence of the high head scarp, the landslide area had already been subject to slope failure events during prehistoric times. As a consequence of this, the processes that take place along and across the slope during lake level variations are affecting an already destabilized slope; this is expected to be more sensitive to variations of the conditions at the slope toe. In general, the presence of artificial lakes can trigger possible seepage process accompanied by an increase in pore water pressure in the slope deposits, with the effect of reducing their shear strength. At the same time, the presence of a water basin may lead to a stabilization of the submerged part of the slope (Paronuzzi et al., 2013). In transient conditions, lake filling or drawdown can trigger landslides (Schuster, 1979; Kenney, 1992; Zhu et al., 2011). In a similar way to the Enguri case, pre-existing, ancient landslides were reactivated during the filling of the water reservoir at the Włocławek dam in Poland (Kaczmarek et al., 2015). This cause-effect relation is even more apparent, where bank-forming materials have a high permeability, like in the study area, in which the slope is mostly made of debris and highly fractured materials; within highly permeable deposits, the reservoir level increase can trigger a rapid reservoir-induced water inflow that reduces both the strength and the factor of safety. This occurred,

https://doi.org/10.5194/essd-2020-324
Preprint. Discussion started: 22 January 2021

for example, at the October 1963 Vajont landslide in NE Italy: As documented by Paronuzzi et al. (2013), among the triggering factors for the disaster, a predominant role was played by reservoir level increase, and by the presence of an already existing landslide. Another example comes from the Byford Creek landslide, located above the Clyde artificial reservoir in New Zealand, where lake filling produced a major increase in deformation rate, followed by long-term creep movements (Macfarlane, 2009).

Our data show that, more than 40 years after the construction of the Enguri reservoir, the slopes still have a high sensitivity to water infilling operations. Moreover, the presence of highly-permeable deposits in the lower part of a slope, as is the case at the Khoko landslide, represents a key aspect to be considered for the assessment of hydrogeological hazard. In such a case, during reservoir level increase, the water pore pressure effects on shear strength prevail over the stabilizing and buttressing effects induced by the water body, resulting in an acceleration in slope movements.

https://doi.org/10.5194/essd-2020-324
Preprint. Discussion started: 22 January 2021

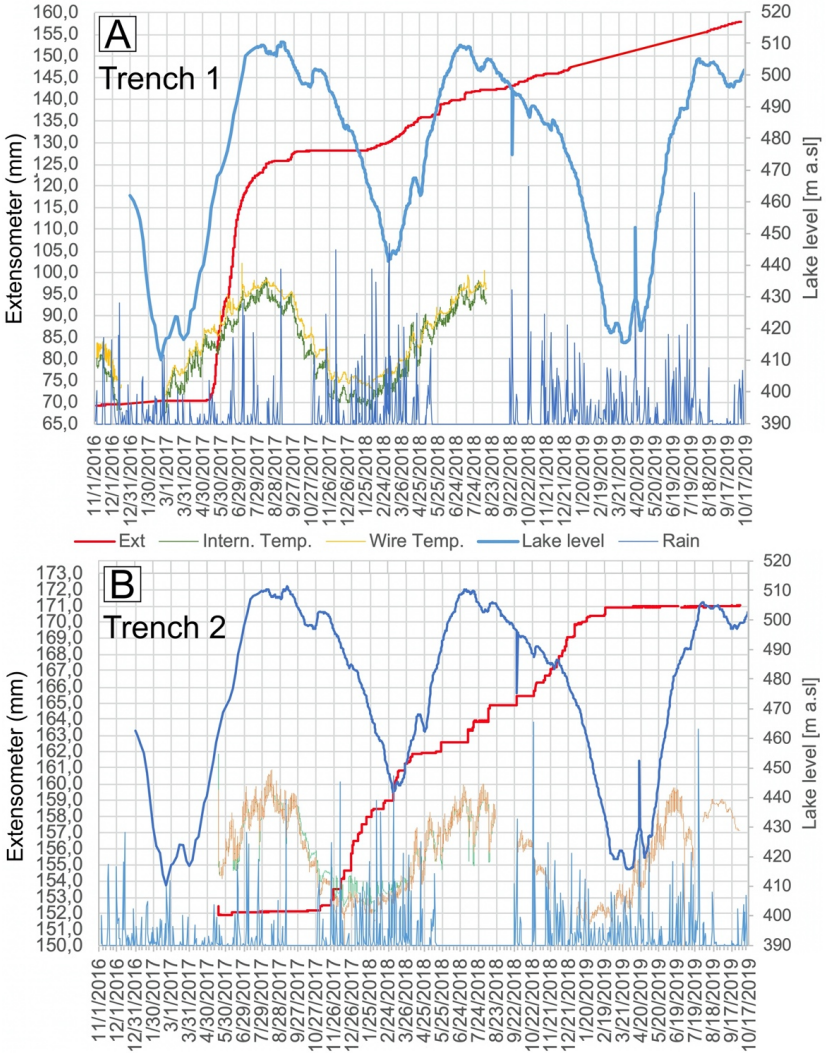

Figure 10. *Graphs showing the combination of all data collected at trench 1 (A) and trench 2 (B).*

6 Data availability

The databases showcased in this work are available for download from the UniData Repository (Milan, Italy) at https://www.unidata.unimib.it/?indagine=deformation-and-meteorological-data-of-the-khoko-landslide-enguri-republic-of-georgia-2016-2020, DOI: 10.20366/unimib/unidata/SI384-1.1 (Tibaldi et al., 2020). The deformation dataset is provided in two separate files, for Trench 1 and for Trench 2, in tab format (deformation data with frequency sampling of 60 min) together with air temperature near the ground surface (frequency sampling of 60 min), and temperature of the extensometer wire in the interior of the instrument (frequency sampling of 60 min). At the same web

https://doi.org/10.5194/essd-2020-324
Preprint. Discussion started: 22 January 2021

335 link is available the file of the meteorological data (frequency sampling of 1 day) and of the lake level
336 variations (frequency sampling each 5 days until 30/7/17 and then each one day).
337

338 **7 Conclusions**

339 At the major Khoko landslide, located on the eastern side of the Enguri artificial water reservoir, a 4-
340 year-long campaign of measurement, by way of two digital extensometers, enables document the
341 activity of the mass movement, at a rate of 8.2 mm/yr to 30.8 mm/yr depending on the site of
342 measurement. During this period, we observed a correlation between rapid infilling of the lake and
343 an increase in deformation rate of the slope. Deformation of the landslide, thus, appears to have been
344 controlled by variations in hydraulic load, induced mainly by lake oscillations. There is a systematic
345 delay between the man-induced lake oscillation and the response of the landslide mass, quantifiable
346 in about one month at extensometer n. 1 and longer at extensometer n. 2. This result, together with
347 the different slip rates at the two instruments, suggest that the Khoko landslide is composed of more
348 than one unstable block, each of which can behave in a different way. Most importantly, the emptying
349 of the lake does not alter landslide stability, despite the related unbuttressing of the slope toe. Rainfall,
350 instead, does not seem to have influence on the pattern of deformation. This overall monitoring effort
351 will help individuate possible future accelerations of deformation at the unstable mass overlooking
352 the Enguri artificial reservoir.

353
354 **Author contributions.** AT coordinated the research and wrote most of the paper. PO designed and
355 maintained the sensor network. FPM and FB contributed to the geological and geomorphological
356 mapping of the landslide area. NT coordinated and contributed to collecting deformation data at the
357 extensometers. LM and JC provided meteorological and lake level data.
358
359 **Competing interests.** The authors declare they have no conflict of interest.
360
361 **Acknowledgements.** We are indebted to the Ministry of Infrastructure of Georgia that helped us to
362 obtain the permission to work along the Jvari-Khaishi-Mestia road.
363
364 **Financial support.** This research was conducted with the financial help from NATO project SfP
365 G4934 "Georgia Hydropower Security", the International Lithosphere Program - Task Force II, and
366 project 216758 of the Shota Rustaveli National Science Foundation. Satellite images were provided
367 in the framework of the European Space Agency project n. 32309 “Active tectonics and seismic
368 hazard of southwest Caucasus by remotely-sensed and seismological data”.
369

370 **References**

371 Bertolini, G., Guida, M., & Pizziolo, M. (2005). Landslides in Emilia-Romagna region (Italy):
372 strategies for hazard assessment and risk management. Landslides, 2(4), 302-312.

https://doi.org/10.5194/essd-2020-324
Preprint. Discussion started: 22 January 2021

373 Bitelli, G., Dubbini, M., & Zanutta, A. (2004). Terrestrial laser scanning and digital photogrammetry
374 techniques to monitor landslide bodies. International Archives of Photogrammetry, Remote Sensing
375 and Spatial Information Sciences, 35(B5), 246-251.

376 Casagli, N., Tibaldi, A., Merri, A., Del Ventisette, C., Apuani, T., Guerri, L., Fortuny-Guasch J. &
377 Tarchi, D. (2009). Deformation of Stromboli Volcano (Italy) during the 2007 eruption revealed by
378 radar interferometry, numerical modelling and structural geological field data. Journal of
379 Volcanology and Geothermal Research, 182(3-4), 182-200.

380 Fell, R., Ho, K. K., Lacasse, S., & Leroi, E. (2005). A framework for landslide risk assessment and
381 management. Landslide risk management, 3-25.

382 Froude, M. J. and Petley, D. N., 2018. Global fatal landslide occurrence from 2004 to 2016, Nat.
383 Hazards Earth Syst. Sci., 18(8), 2161–2181, doi:10.5194/nhess-18-2161-2018.

384 Gulen L., and EMME WP2 Team (2011). Active faults and seismic sources of the Middle East region:
385 earthquake model of the Middle East (EMME) project. In: Abstracts of the AGU Fall Meeting, San
386 Francisco, California, 5-9 December 2011.

387 Kaczmarek, H., Tyszkowski, S., and Banach, M., 2015. Landslide development at the shores of a
388 dam reservoir (Włocławek, Poland), based on 40 years of research, Environmental Earth Sciences,
389 74(5), 4247-4259.

390 Kenney, T.C., 1992. Slope stability in artificial reservoirs: influence of reservoir level, selected cases,
391 and possible solutions, In: Semenza, E., Melidoro, G. (Eds.), Proceedings of the meeting on the 1963
392 Vajont landslide, 17-19 September 1986, Ferrara, Cansiglio and Vajont. Grafica Ferrarese, Ferrara,
393 Italy, 67-85.

394 Koçyigit, A., Yılmaz, A., Adamia, S., and Kuloshvili, S. (2001). Neotectonics of East Anatolia
395 Plateau (Turkey) and Lesser Caucasus: Implication for transition from thrusting to strike-slip faulting.
396 Geodin. Acta, 14, 177-195.

397 Liu Shao-tang 2006. Deformation measurements during the construction of large dam projects.
398 Chinese Journal of Underground Space and Engineering 06(Z2): 1346–1348.

399 Liu, S. T., and Wang, Z. W. (2008). Choice of surveying methods for landslides monitoring. In
400 Landslides and engineered slopes: from the past to the future. Proceedings of the tenth international
401 symposium on landslides and engineered slopes. Taylor & Francis, Xi'an.

402 Macfarlane, D.F., 2009. Observations and predictions of the behaviour of large, slow-moving
403 landslides in schist, Clyde Dam reservoir, New Zealand, Engineering Geology, 109(1-2), 5-15.

404 Paronuzzi, P., Rigo, E., and Bolla, A., 2013. Influence of filling–drawdown cycles of the Vajont
405 reservoir on Mt. Toc slope stability, Geomorphology, 191, 75-93.

406 Pasquaré Mariotto F., Tibaldi A. (2016). nversion kinematics at deep-seated gravity slope
407 deformations revealed by trenching techniques. Nat. Hazards Earth Syst. Sci., 16, 663-674.

408 Pasquaré, F., Tormey, D., Vezzoli, L., Okrostsvaridze, A., Tutberidze, B. (2011). Mitigating the
409 consequences of extreme events on strategic facilities: Evaluation of volcanic and seismic risk
410 affecting the Caspian oil and gas pipelines in the Republic of Georgia. J. Environ. Man., 92, 1774–
411 1782.

412 Reilinger, R. E., McClusky, S. C., Oral, M. B., King, R. W., Toksoz, M. N., Barka, A. A., Kinik, I.,
413 Lenk, O., and Sanli, I. (1997). Global Positioning System measurements of present-day crustal
414 movements in the Arabia-Africa-Eurasia plate collision zone. J. Geophys. Res., 102, 9983–9999.

415 Reilinger, R. E., McClusky, S. C., Vernant, P., Lawrence, S., Ergintav, S., Cakmak, R., Ozener, H.,
416 Kadirov, F., Guliev, I., Stepanian, R., Nadariya, M., Hahubia, G., Mahmoud, S., Sakr, K., Arrajehi,
417 A., Paradissis, D., Al-Aydrus, A., Prilepin, M., Guseva, T., Evren, E., Dmirotsa, A., Filikov, S. V.,

https://doi.org/10.5194/essd-2020-324
Preprint. Discussion started: 22 January 2021

418 Gomez, F., Al-Ghazzi, R., Karam, G. (2006). GPS constraints on continental deformation in the
419 Africa-Arabia-Eurasia continental collision zone and implications for the dynamics of plate
420 interactions. J. Geophys. Res., 111, B05411, https://doi.org/10.1029/2005JB004051.

421 Schuster, R.L., 1979. Reservoir-induced landslides, Bulletin of the International Association of
422 Engineering Geology, 20, 8-15.

423 Spiker, E. C., & Gori, P. (2003). National landslide hazards mitigation strategy, a framework for loss
424 reduction (No. 1244). US Geological Survey.

425 Tibaldi, A., Pasquaré F. (2008). Quaternary deformations along the "Engadine–Gruf tectonic
426 system", Swiss–Italian border. J. Quaternary Sci., 23 475–487.

427 Tibaldi, A., Rovida, A., Corazzato C. (2004). A giant deep-seated slope deformation in the Italian
428 Alps studied by paleoseismological and morphometric techniques. Geomorphology, 58, 27–47.

429 Tibaldi, A., Corazzato, C., Rust, D., Bonali, F. L., Pasquaré Mariotto, F., Korzhenkov, A. M., Oppizzi
430 P., and Bonzanigo, L. (2015). Tectonic and gravity-induced deformation along the active Talas–
431 Fergana Fault, Tien Shan, Kyrgyzstan. Tectonophysics, 657, 38–62.

432 Tibaldi, A., Alania, V., Bonali, F. L., Enukidze, O., Tsereteli, N., Kvavadze, N., Varazanashvili, O.
433 (2017a). Active inversion tectonics, simple shear folding and back-thrusting at Rioni Basin, Georgia.
434 J. Struct. Geol., 96, 35–53.

435 Tibaldi, A., Russo, E., Bonali, F.L., Alania, V., Chabukiani, A., Enukidze, O., Tsereteli, N. (2017b).
436 3-D anatomy of an active fault propagation fold: a multidisciplinary case study from Tsaishi
437 (Georgia), western Caucasus. Tectonophysics, 717, 253–269.

438 Tibaldi, A., Korzhenkov, A.M., Pasquaré Mariotto, F., Rust, D., Tsereteli, N. (2018). NATO and
439 earth scientists: An ongoing collaboration to assess geohazards and contribute to societal security in
440 Central Asia and the Caucasus. Episodes, 41, 193-205.

441 Tibaldi, A., Oppizzi, P., Gierke, J. S., Oommen, T., Tsereteli, N., Gogoladze, Z. (2019). Landslides
442 near Enguri dam (Caucasus, Georgia) and possible seismotectonic effects. Natural Hazards and Earth
443 System Sciences, 19, 71.

444 Tibaldi, A., Oppizzi, P., Bonali, F., Pasquarè Mariotto, F., Tsereteli, N., Mebonia, L., 2020.
445 Deformation and meteorological data of the Khoko landslide, Enguri, Republic of Georgia. UniData
446 - Bicocca Data Archive, Milan. Study Number SI384, Data file version 1.0 DOI:
447 10.20366/unimib/unidata/SI384-1.1

448 Tsereteli, N., Tibaldi, A., Alania, V., Gventsadse, A., Enukidze, O., Varazanashvili, O., Müller B. I.
449 R. (2016). Active tectonics of central-western Caucasus, Georgia. Tectonophysics, 691, 328-344.

450 Varazanashvili, O., Tsereteli, N., Bonali, F. L., Arabidze, V., Russo, E., Pasquaré Mariotto, F.,
451 Gogoladze, Z., Tibaldi, A., Kvavadze, N., Oppizzi, P. (2018). GeoInt: the first macroseismic intensity
452 database for the Republic of Georgia. J. Seismol., 1–43, https://doi.org/10.1007/s10950-017-9726-5.

453 Zhu, D., Yan, E., Hu, G., and Lin, Y. 2011. Revival deformation mechanism of Hefeng Landslide in
454 the Three Gorges Reservoir based on FLAC3D software, Procedia Engineering, 15, 2847-2851.